

NCAR/TN-370+STR
NCAR TECHNICAL NOTE

February 1992

A SPECTRAL VEGETATION RADIOMETER FOR AIRBORNE BOUNDARY-LAYER RESEARCH

RESEARCH AVIATION FACILITY
ATMOSPHERIC TECHNOLOGY DIVISION

NATIONAL CENTER FOR ATMOSPHERIC RESEARCH
BOULDER, COLORADO

A Spectral Vegetation Radiometer for Airborne Boundary-Layer Research

Lutz Bannehr

**Advanced Study Program of the Office of the Director, and
Research Aviation Facility of the Atmospheric Technology Division
National Center for Atmospheric Research (NCAR), Boulder, CO 80307-3000**

Vince Glover

**Research Aviation Facility of the Atmospheric Technology Division
National Center for Atmospheric Research (NCAR), Boulder, CO 80307-3000**

February 1992

CONTENTS

List of Figures	v
List of Tables	vii
Preface	ix
Acknowledgements	xi
Abstract	xiii
1 BACKGROUND	1
2 SPECTRAL VEGETATION RADIOMETER (SVR)	5
3 CALIBRATION	12
3.1 Optical Air Mass	12
3.2 Langley Analysis	14
3.3 Calibration Program	19
4 OBSERVATIONS AND APPLICATIONS	22
5 Summary	30
References	31
Appendix A: VEGCAL program	32

LIST OF FIGURES

	PAGE
1.1 Spectral response of the NOAA-AVHRR radiometer filters for the channels 1 and 2, and the spectral reflectance of different natural surfaces. Figure is redrawn from Blümel <i>et al.</i> (1988).	2
2.1 Geometry of a sunphotometer according to the W.M.O. guidelines.	5
2.2 Picture of the Spectral Vegetation Radiometer SVR.	10
3.1 Calibration time required for an air mass range of four throughout the year.	15
3.2 Langley plot of the three wavelengths of the spectral vegetation radiometer.	16
4.1 Time series of radiometrically measured surface temperature and derived vegetation index NDVI in the Greely area, Colorado.	24
4.2 High rate vegetation index time series.	26
4.3 High rate NDVI time series of the Riverside Reservoir, Colorado.	27
4.4 Example of data from the spectral vegetation radiometer, identifying shade projected by clouds on the surface.	29

LIST OF TABLES

PAGE

2.1	Basic characteristics of the spectral vegetation radiometer SVR.	11
-----	--	----

PREFACE

This Technical Note presents a comprehensive description of the Spectral Vegetation Radiometer (SVR) used on NCAR aircraft to derive information about the vegetation cover. The information presented here is more detailed than is possible in a Journal article. The Tech. Note is structured to first provide the reader with background information of the vegetation index. Next, applications are discussed, and finally the problems involved in analyzing the vegetation index are described. Furthermore, the reader obtains an inside view of the instrument design and how the calibration should be performed. The examples of the spectral vegetation radiometer presented, explore the utility of remote sensing methods for meteorological research in the planetary boundary layer.

This research has been supported by the National Science Foundation.

A handwritten signature in black ink, reading "Lutz Bannehr". The signature is written in a cursive style with a large, prominent 'L' and 'B'.

Lutz Bannehr

February 1992

ACKNOWLEDGEMENTS

The authors would like to thank Aref Nammari, Dave McFarland, Diana Rodgers of the NCAR Research Aviation Facility (RAF) and Michl Howard of the NCAR Design and Fabrication Service section for their assistance during the development of the spectral vegetation radiometer. The authors are indebted to Larry Radke and Darrel Baumgardener of the RAF for their generous financial support.

ABSTRACT

Sensible and latent heat fluxes determined from airborne measurements are widely used in turbulence research and boundary layer investigations. These fluxes are strongly modified by the surface vegetation cover and moisture content. Therefore, a high spatial resolution indicator of the surface cover is of great importance for micro-meteorological investigations. A Spectral Vegetation Radiometer (SVR), based on the vegetation radiometer developed by Bannehr (1990), was rebuilt and modified to overcome the instrumental deficiencies of previous devices and to facilitate airborne investigations of the vegetation cover. The instrument is a three wavelength radiometer. It permits observers to distinguish between vegetated and non-vegetated surfaces, to identify areas which are partially covered by clouds, and to identify algae on water. The design of the vegetation radiometer and the examples presented demonstrate the performance of the SVR and the potential of it for airborne boundary layer research.

1 BACKGROUND

Vegetation has chlorophyll absorption bands in the visible spectrum from 400-680 nm (photosynthetic active radiation) where the incident radiation is absorbed and scattered by the photosynthetic pigment in the leaves. For wavelengths between 680 and 750 nm, the absorption decreases by three to four times, stabilizing at longer wavelengths towards the infrared. In the near infrared, plants have no chlorophyll absorption bands a characteristic which prevents them from overheating. Ground that is not covered by vegetation does not show a large variability in spectral reflectance with wavelength. The reflectance increases with wavelength in an almost linear fashion, the slope depending upon the soil type and the surface moisture. These different spectral characteristics of photosynthetically active plants and other surface types make it possible to classify the ground cover. Most of the work done on vegetation discrimination uses data from the first two channels of the Advanced Very High Resolution Radiometer (AVHRR) of the NOAA polar-orbiting satellites. These two channels are in the visible and near infrared. Their spectral transmission and bandwidths are shown in Figure 1.1, along with the spectral reflectance of different natural surfaces. Occasionally the simple difference of signals between the two channels are used as vegetation index, with a large difference corresponding to a high vegetation index and a small difference corresponding to a small vegetation index.

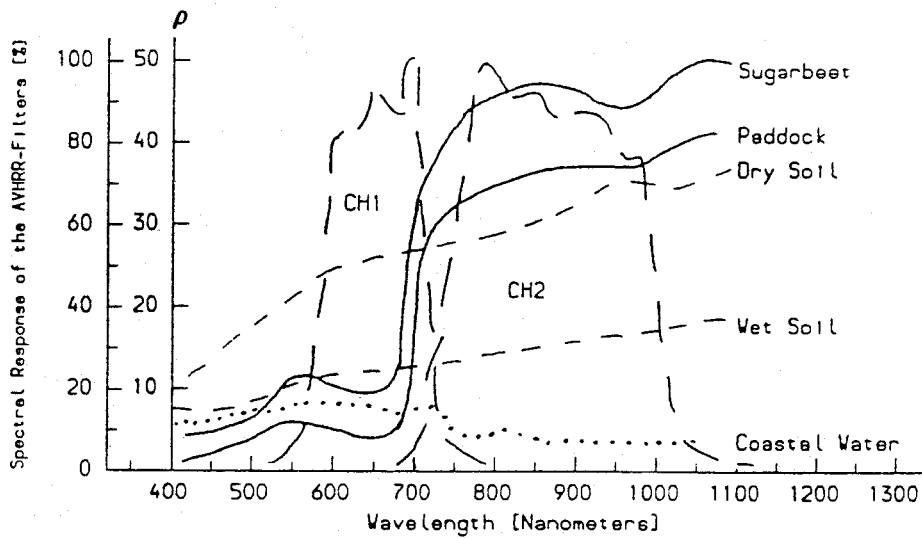


Fig. 1.1 Spectral response of the NOAA-AVHRR radiometer filters for the channels 1 and 2, and the spectral reflectance of different natural surfaces. Figure is redrawn from Blümel et al. (1988).

However, the parameter most frequently used for categorization of the state of the vegetation is the Normalized Difference Vegetation Index (NDVI). This vegetation index is defined as:

$$NDVI = \frac{\rho_2 - \rho_1}{\rho_2 + \rho_1} \quad (1.1)$$

where ρ_1 and ρ_2 are the reflectances of vegetation inside and outside the chlorophyll absorption bands. The denominator in Equation 1.1 is a normalization factor, which partially compensates for the difference in the surface reflectance associated with solar elevation or satellite viewing angles.

Apart from obtaining information about the state of the vegetation, the NDVI has been related to the leaf area index (LAI) up to a value of 2 (Sellers, 1985). Further investigations showed that the NDVI is almost directly proportional to the absorbed Photosynthetic Active Radiation (PAR). Tucker *et al.* (1986) demonstrated a relationship between the atmospheric carbon dioxide concentration at the surface and the vegetation index, and Hope and McDowell (1990) used a relation between the surface temperature and the spectral vegetation index for the evaluation of heat fluxes. Paltridge and Barber (1988) modified the NDVI derived from NOAA-AVHRR data and related the resultant parameters to the "grassland" fuel-moisture content in order to obtain an operational system for fire ban declarations by the Country Fire Authority of Victoria (Australia). Apart from the investigations of Tucker *et al.* (1986), the vegetation index has always been derived from satellite data.

For micro-meteorological research in the boundary layer, introducing the remotely sensed vegetation parameter will contribute valuable information. The additional information will strengthen the understanding of the processes involved in controlling the energy budget and will help in understanding the impact the destruction of vegetation has on the climate.

Bolle (1990) addressed the problems encountered when determining the vegetation index. Difficulties arise in intercomparing the work of different authors because of

- 1) the current lack of an agreed standard for the spectral bands and bandwidths used,
- 2) the dependence of the reflectance on the solar altitude,

- 3) the absence of a reference for normalization of the vegetation index is missing,
- 4) the angle dependence of the scattered and reflected radiation, and
- 5) non-standard definitions of the vegetation index.

Geometric and atmospheric corrections must be applied when deriving the vegetation index from orbiting satellite data. Employing the vegetation radiometer on low-flying aircraft to determine the vegetation index reduces some uncertainties. For instance, there are no atmospheric corrections required and no geometrical correction necessary because the instrument can be installed such that it always remains in nadir position. Scenery effects which are caused by a non nadir positioned instrument are small. A further good feature of the SVR for boundary layer research is that even under cloudy conditions the radiometer provides information about the vegetation cover. Given the fast time response of the instrument of 24 ms the spatial resolution, especially when flying low, is so high that even single bushes can be detected.

2 SPECTRAL VEGETATION RADIOMETER (SVR)

The spectral vegetation radiometer (SVR) is a three wavelength device. Since it is basically a sunphotometer, the design of the SVR follows the guidelines of the W.M.O. (1986) for the construction of sunphotometers. The geometry of the radiometer is illustrated in Figure 2.1.

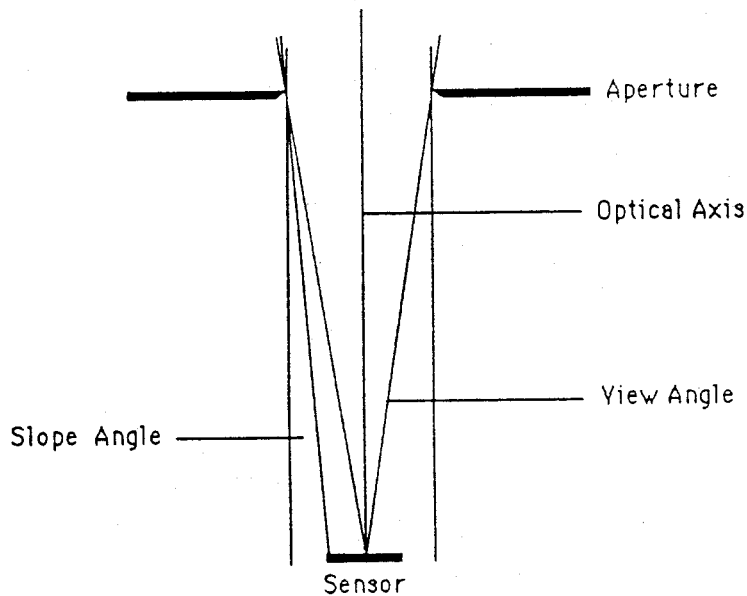


Fig. 2.1 Geometry of a sunphotometer according to the W.M.O. guidelines.

According to the recommendations, the field of view of the instrument should be small in order to minimize the measurement of the circumsolar or aureole radiation. An opening

angle of 2.5° and a slope angle of 1° is satisfactory for the measurements. The equations that satisfy the recommendations can be written as follows:

$$a = \frac{R}{r} \quad (2.1)$$

$$b = \frac{L}{r} \quad (2.2)$$

$$z_0 = \tan^{-1}\left(\frac{a}{b}\right) \quad (2.3)$$

$$z_p = \tan^{-1}\left(\frac{a-1}{b}\right) \quad (2.4)$$

r = radius of receiver

R = radius of limiting aperture

L = distance between the receiver aperture and limiting aperture

z_0 = opening angle

z_p = slope angle

The WMO recommends that the opening angle should be $\leq 4^\circ$. Furthermore, the slope angle should be $1^\circ \leq z_p \leq 2^\circ$ and $b \geq 15$.

The SVR uses a light barrel for each of the three sensors. Each of these is filtered at different wavelengths. The opening angle is 2.3° . The three light tubes are anodized in black color to reduce internal scattering. No focusing lenses are required for the instrument. Ultraviolet enhanced silicon photo diodes are used as sensors. These devices have a higher output signal than common silicon photo diodes. The silicon detector is operated, in the unbiased photovoltaic mode while the amplifier is operated in the inverted common mode. Attached to the top of each sensor is an interference filter with a half bandwidth of 10 nm. A quasi-monochromatic bandwidth is essential in order to calibrate the instrument by the ratio-Langley technique, described below. The nominal wavelengths chosen for the radiometer are 650, 760 and 862 nm. At 650 nm extinction occurs by molecules, aerosols and ozone. This wavelength is close to a maximum of the chlorophyll absorption band. At 760 and 862 nm the radiance signals are affected by molecular scattering and aerosol extinction. These two wavelengths are outside the chlorophyll absorption bands of plant leaves and needles. As mentioned above, only two wavelengths are required to derive the vegetation index, one inside and one outside of the chlorophyll absorption band. The 760 nm wavelength is included only for research purposes and the examples of the vegetation index presented in this Tech. Note are determined only from the 650 and 862 nm wavelengths. Another benefit from choosing these wavelengths, is the exclusion of the influence of the highly variable water vapor. In order to achieve a better resolution, the instrument can be operated in two amplification modes. One mode is used to measure the low radiance signals; the other is required for calibration purposes or if the device is operated as a sunphotometer.

The difference between the gains of the two operation modes is determined by the ratio of the feedback resistors ($R1/R2$) used in the high- and low-gain configurations. Therefore, when the calibration is performed in the high intensity mode and the measurements are later on carried out in the low intensity mode, the observed voltages have to be multiplied by the gain factor $G=R1/R2$.

Each of the three light tubes of SVR has two apertures. One is the sensor aperture and the other limits the field-of-view (upper aperture). The upper aperture can be replaced by different sizes to have the option of various opening angles. A glass plate is fitted underneath the upper aperture to seal the instrument from moisture, dust and dirt which could affect the performance of the radiometer. The interference filters are located above the sensor apertures. The three signals are recorded separately, each on one analog channel of the aircraft data acquisition system. The vegetation parameter is calculated from the signals during post-flight data processing.

The silicon detectors have a temperature-dependent sensitivity. With increasing temperature the response of the shorter wavelength (<550 nm) detector decreases whereas the response in the near infrared (>860 nm) detector increases (EG & G Judson, 1990). Also, the transmittance of the interference filters depends on the temperature. The central wavelength of the filters changes at a rate of 0.018 nm/ $\Delta^{\circ}\text{C}$ (Omega Optical Inc., 1990). This effect can be regarded as small for the interference filters used and the applications.

Therefore, for a wide range of temperatures compensation electronics are not necessary. The radiometer is installed inside the aircraft so that the temperature of the instrument is close to the cabin temperature. Thus, the effect of temperature on the sensors, interference filters and electronic components is minimized and it is not necessary to provide for temperature control. The time response (0 - 99%) of the spectral vegetation radiometer was determined to be 24 ms. Figure 2.2 shows the spectral vegetation radiometer.

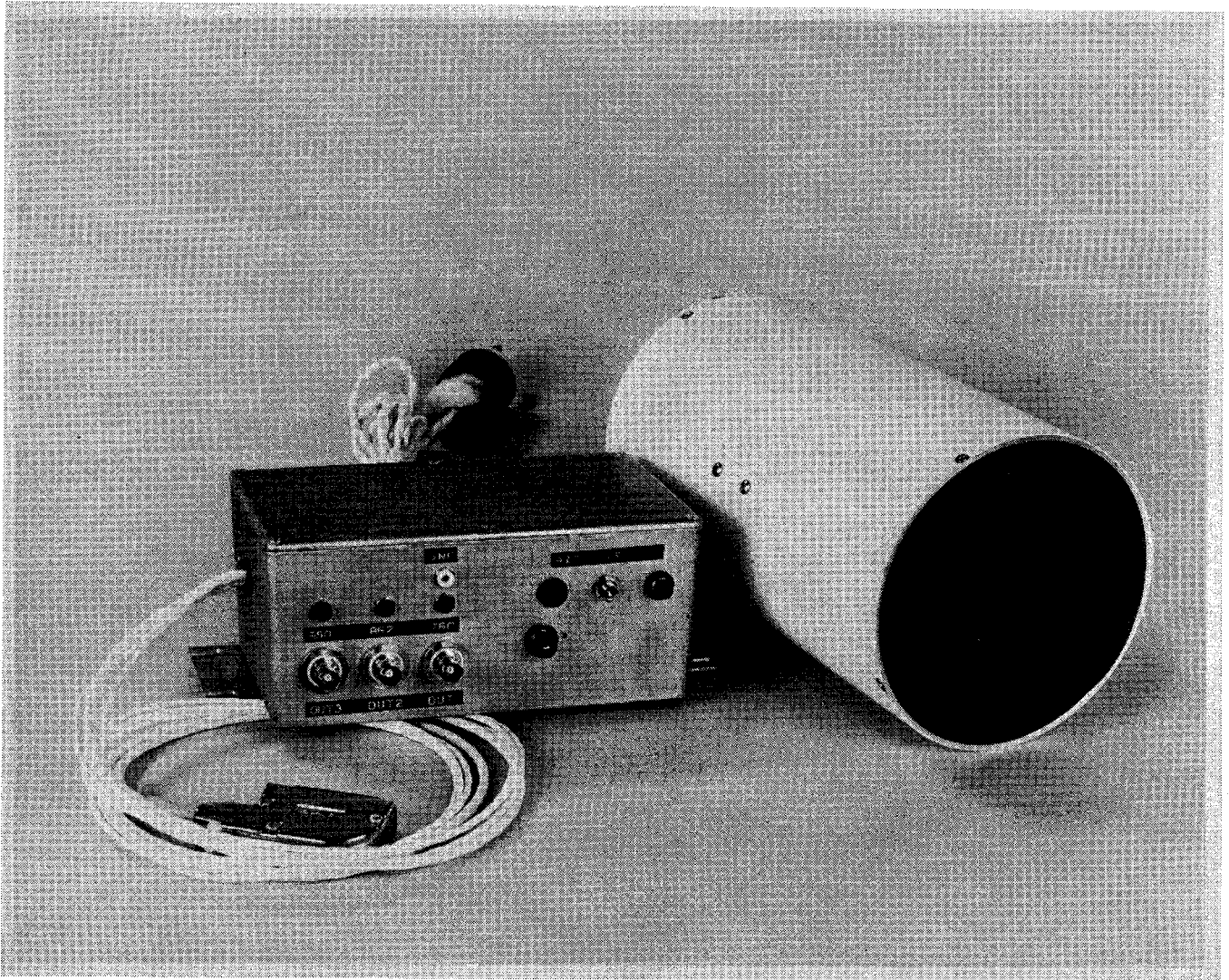


Fig. 2.2 Picture of the spectral vegetation radiometer SVR.

Table 2.1 Basic characteristics of the spectral vegetation radiometer SVR.

General Description:

Three wavelength radiometer to facilitate airborne investigations of surface cover.

Size:

diameter : 140 mm

height : 270 mm

weight : 5 kg

opening angle : 2.3°, variable by changing apertures

Sensor: : UV-BG 215 BQ silicon UV-enhanced photodiode

active area : 23.4 mm²

spectral response : 250 - 1150 nm

time response : ~100 ns

Interference Filters:

nominal wavelengths : 650 nm, 760 nm and 862 nm

bandwidth : 10 nm

Instrument Time Response:

response from 0% to 99% : 24 ms

Output:

0V to 5V, for each channel

Power:

±9V, 30 mA, operation either batteries or 110V

Calibration:

ratio-Langley technique

Application:

The SVR allows investigators to distinguish between different photosynthetically active surfaces such as lush vegetation, sparsely vegetated surfaces, soil, and water. It detects shaded areas on the ground caused by clouds.

3 CALIBRATION

3.1 Optical Air Mass

In order to perform the Langley calibration the optical air mass must be known. The optical air mass, m , gives the number of vertical atmospheres equivalent to the direct path through the atmosphere. Kasten (1966) introduced the relative optical air mass which can be represented by:

$$m = \frac{1}{(\sin \theta' + a(\theta' + b)^{-c})} \quad (3.1)$$

θ' = observed sun elevation (true sun elevation plus refraction)
 a = 0.150
 b = 3.885
 c = 1.253

He uses the refractive index of air for 700 nm (center point of the incoming solar energy) of the ARDC-Atmosphere, introduced in 1959. The relative optical air mass for each atmospheric species component is different. For water vapor Kasten (1966) gives the following constants:

$$a = 0.0548; \quad b = 6.379; \quad c = 1.452.$$

Since the aerosol concentration profile is closely connected to the water vapor profile, for most cases, the relative optical air mass for turbid air, m_a , can be set equal to the relative optical air mass of water vapor, m_w . To derive the relative optical air mass for ozone, m_o , Robinson (1966) assumed the existence of a mean vertical distribution with a maximum concentration at 20 to 25 km height. The equation for ozone optical air mass can then be expressed from geometrical considerations:

$$m_o = \frac{1 + a}{(\sin^2\theta + 2a)^{0.5}} \quad (3.2)$$

$$a = 23/6378 = 3.606 \cdot 10^{-3}$$

The ratio 23/6378 is the relation between the mean height of the ozone layer (23 km) and the radius of the earth (6378 km).

The calibration factor is derived later using the weighted relative optical air mass m_r , which is defined as:

$$m_r = \frac{\sum m_i \tau_i}{\sum \tau_i} \quad (3.4)$$

where m_i is the species optical air mass and τ_i atmospheric species optical depth.

3.2 Langley Analysis

Since the SVR is basically a sunphotometer, the calibration procedure is identical to that for sunphotometers. The technique for obtaining a calibration coefficient for a sunphotometer is the Langley technique based on the Bouguer-Lambert-Beer law which can be related as:

$$\ln V = \ln V_0 - \tau m \quad (3.3)$$

This method requires direct measurements of the SVR output voltage, V , under clear, stable sky conditions for a range of air masses, m . By extrapolating the logarithm of the direct signal V to an air mass of zero, one obtains the calibration factor V_0 . The quantity τ in Equation 3.3 denotes the optical depth. Forgan (1988) suggested that the calibration should be performed over the shortest possible time but over at least a three air mass range. Data should be taken between air masses $2 < m < 6.5$. Figure 3.1 shows the time of day during which the calibration should be done and the time it takes to perform the calibration over four air masses at a latitude of 40°N either in the morning or afternoon. For example, on day 180 the calibration should be done either between 5:34 and 7:04 or between 16:52 and 18:22.

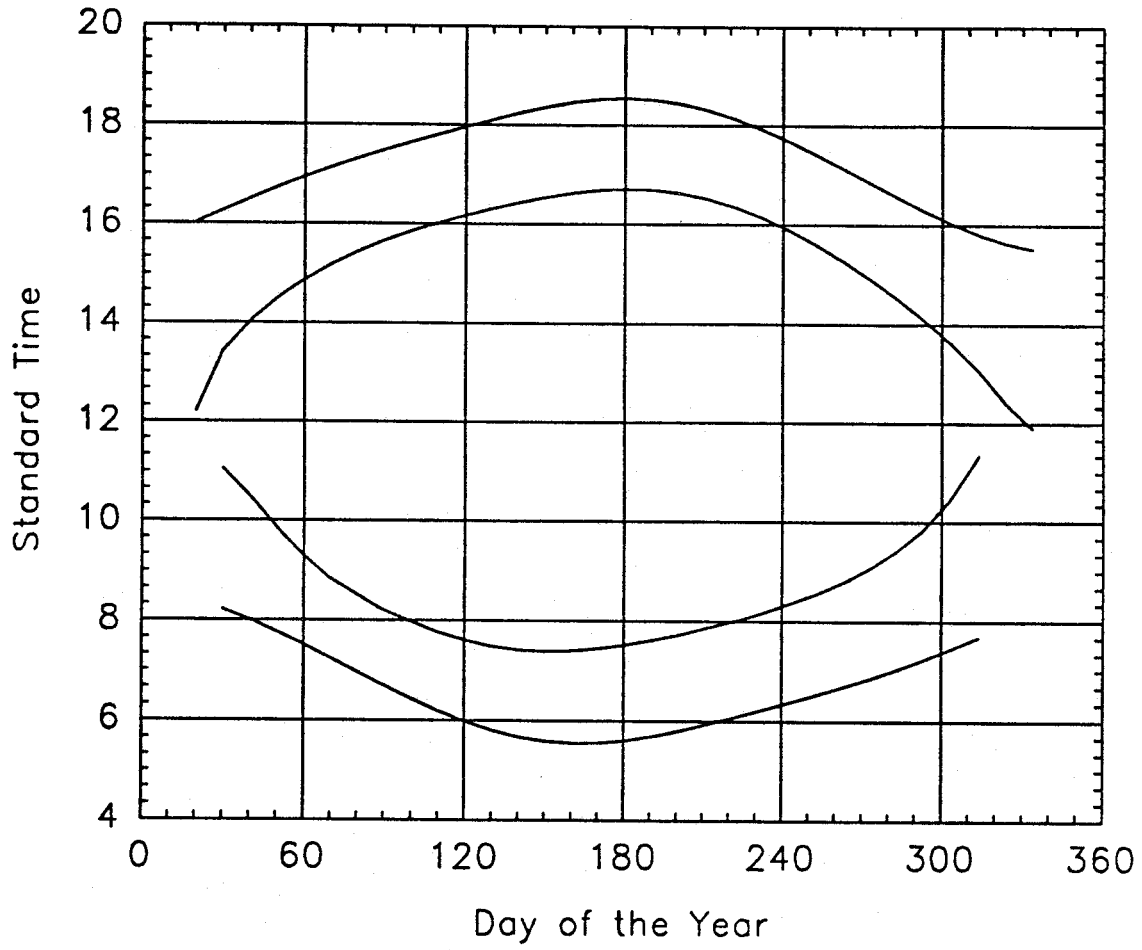


Fig. 3.1 Calibration time required for an air mass range of four throughout the year.

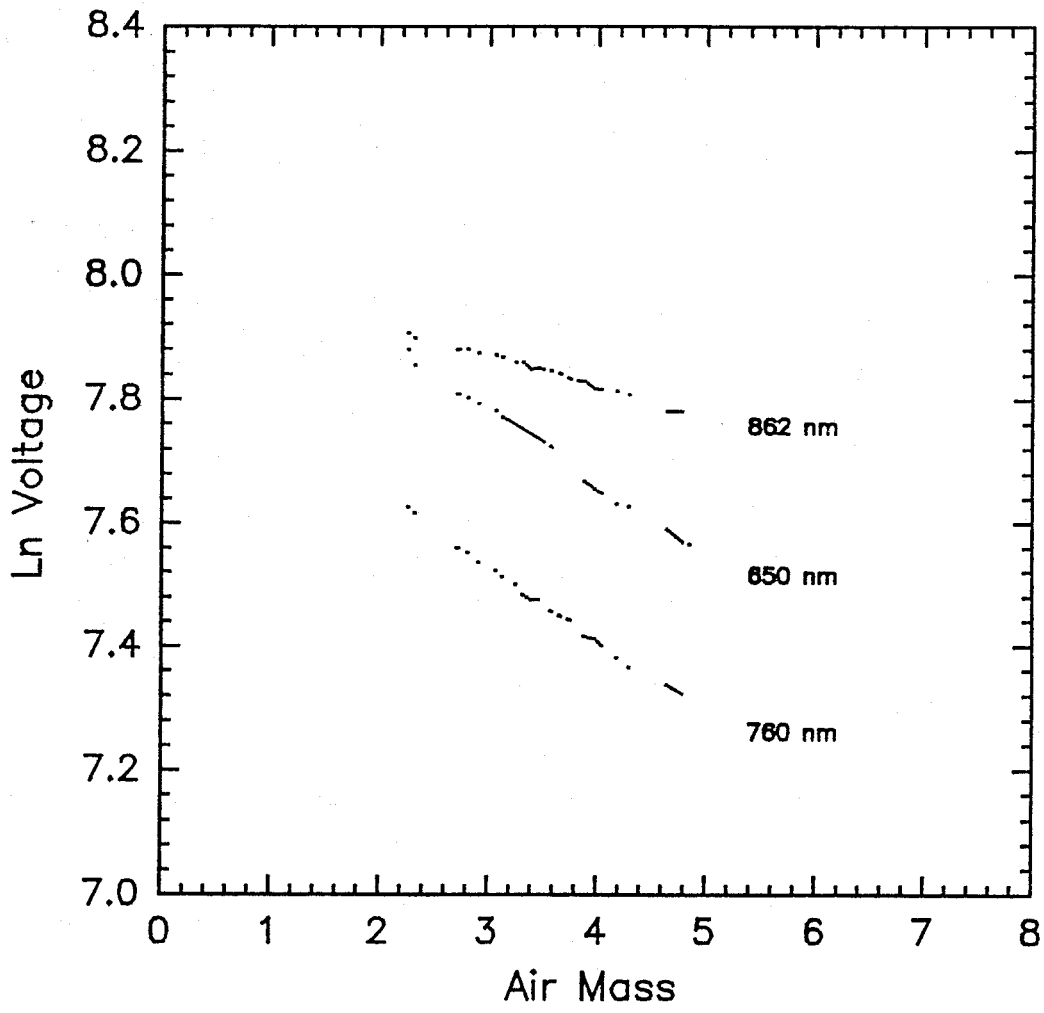


Fig. 3.2 Langley plot of the three wavelengths of the spectral vegetation radiometer.

Figure 3.1 shows an example of the Langley analysis. The logarithm of the direct signal is only a linear function of the air mass if the optical depth, τ , does not change during the calibration procedure. The presumption of this simple method, a temporarily invariant atmosphere over four air masses (2-6), is rarely available. Effects caused by the variability of the atmosphere can be reduced if the calibration is made from high altitude stations (Fröhlich and London, 1986).

Shaw (1976) discussed the instrumental and calibration problems of sunphotometers and concluded that instrumental errors are small compared to calibration errors. He also discussed the possibility of using standard lamps for the calibration. Unfortunately, the scale of lamps spectral irradiance is still too inaccurate for regions with low aerosol optical depth, but artificial lamps can be employed for monitoring long-term stability.

For a Langley analysis the error caused by small changes in the aerosol optical depth during the calibration period can have a large impact on the derived calibration factor. The error in I_0 is given by:

$$\Delta I_0 = \frac{m_1 m_2}{m_1 - m_2} [\tau(m_1) - \tau(m_2)] \quad (3.5)$$

where m_1 and m_2 are the air masses for the first and last samples taken. The quantities $\tau(m_1)$ and $\tau(m_2)$ are the optical depth at the beginning and end of the period. For instance, assuming a change in the optical depth from $\tau(m_1)$ to $\tau(m_2)$ by only 0.005 for the air masses from 2 to 6 results in an error in the calibration coefficient of 1.5%. However, the lack of a need for an absolute radiance calibration makes it possible to use the ratio-Langley technique as described by Forgan (1988). By forming the ratio I_{01}/I_{02} , the effect of atmospheric variability is minimized and the bias error of the ratio is found to be less than the smallest bias of the individual wavelengths. The relative radiance L_1' measured at wavelength 1 in terms of wavelength 2 is:

$$L_1' = \frac{I_{12}}{C_{12}} S_1. \quad (3.6)$$

In this expression I_{12} is the ratio of the spectral solar irradiances for the two SVR wavelengths at the top of the atmosphere:

$$I_{12} = \frac{I_{01}}{I_{02}}. \quad (3.7)$$

S_1 in Equation 3.6 is the measured signal; and C_{12} is the ratio-Langley calibration.

$$C_{12} = \frac{S_{01}}{S_{02}} \quad (3.8)$$

The relative $NDVI_v$ as calculated from the data of the SVR is then determined by:

$$NDVI_v = \frac{L_2 - L_1'}{L_2 + L_1'} \quad (3.9)$$

3.3 Calibration Program

A computer routine has been written to determine the individual calibration coefficients for each wavelength via a least squares analysis as well as the ratio-Langley calibration coefficients. In order to minimize erroneous data used for the least squares fit, the computer routine contains a statistical iterative filter, allowing the operator to reject iteratively all unwanted values of the observations above or below a specified standard deviation. The SVR was calibrated on 17 September 1991 before the first test flight was undertaken. The calibration program which is called VEGCAL is written in Fortran 77 and is listed in Appendix A. Before the VEGCAL can be run, a reader file must be created which contains the following data:

```
HDR1
HDR2
DAY, MONTH, YEAR, LONG, LAT, ZONE, P, FEET
OFFSET(WV650), OFFSET(WV760), OFFSET(WV862), THRES
OM_L1, OM_L2
TIME, WV650, WV760, WV862

"      "      "      "
"      "      "      "
"      "      "      "
```

HDR1 and HDR2 are user comment lines, where each line should not exceed 80 characters.

DAY, MONTH, YEAR is the date the observation were made. LONG and LAT denote the

geographic longitude and latitude of the calibration station. The ZONE parameter describes the time from Greenwich Mean Time in fraction of hours (e.g. 9.5). P and FEET are the pressure and feet at the calibration station. In the next line the offset of each individual wavelength must be provided. Also in the same line the parameter THRES is specified. All observed data above THRES multiplied by the standard deviation are iteratively rejected. In the following line the air mass limits (OM_L1 and OM_L2) are defined. In the subsequent lines the time (TIME) and the observed voltages of the individual wavelengths (WV650, WV760 and WV862) appear. The following is a list of the results of a calibration processed by the VEGCAL program.

RESULTS OF THE CALIBRATION

=====

Date = 17/9/1991
Longitude = -105.12
Latitude = 39.95
Air mass a = 2.178
Air mass b = 4.887
Total Observations = 54

Least Squares Analysis Individual Calibration Factors

Observations : 41
V0_650 : 3456.12
tau_650 : 0.11870
sdev_650 : 0.0077

Observations : 46
V0_760 : 2706.26
tau_760 : 0.12129
sdev_760 : 0.0051

Observations : 42
V0_862 : 3070.08
tau_862 : 0.04963
sdev_862 : 0.0040

Ratio-Langley Calibration

These factors must be multiplied by the 650 and 862 nm signals

C_650 : 1.0007
C_862 : 0.7097

4 VEGETATION OBSERVATIONS AND APPLICATIONS

A test flight was carried out on 3 October 1991 north of Denver, Colorado, USA. The flight was accomplished in an area of manifold surface types, some being dense green vegetation. The performance of the SVR was evaluated using a downward-facing video camera together with the Precision Radiation Thermometer (PRT-5 radiometer), measuring the surface temperature in the spectral bandwidth between 9.5 and 11.5 μm . All three devices were mounted in the body of the NCAR King Air Beechcraft aircraft. Care was taken to ensure alignment of all instruments to the nadir. A second video camera was installed in the cockpit pointing in flight direction. Given the SVR opening angle of 2.3° and a cruising altitude of 110 m, the circular area resolved at the ground is approximately 4.4 m in diameter. The opening angle of the PRT-5 is 2° . The sampling rate of the three wavelengths were 50 Hz and filtered with a cutoff frequency of 10 Hz. The time constant of the PRT-5 is 0.5 sec. During the observations the PRT-5 data were sampled at 10 Hz and filtered at 1 Hz. The oversampling is required to prevent aliasing. Flying at a mean true air speed of 87 m/s and a 10 Hz cutoff frequency for the SVR results in one data point every 8.7 m. This implies that single trees can still be detected.

The objective of the following paragraphs is to provide the user with examples of the SVR rather than to analyze the data in detail. The normalized vegetation index NDVI presented was calculated from the observed radiance signals at 650 and 862 nm.

Figure 4.1 shows the NDVI and the bolometric measured surface temperature. Each sample represents 1 sec flight time; thus, a time span of 20 minutes is displayed in Figure 4.1. High values of the $NDVI_v$ imply high vegetation. The radiometrically measured surface temperature also gives some information about the underlying ground; under clear skies, green vegetation has a lower temperature than non-vegetated surfaces. However, as it can be seen in Figure 4.1 and demonstrated later, the surface temperature does not enable a differentiation between water and green vegetation. With the spectral vegetation radiometer the ground cover can be resolved clearly. Upspikes in the NDVI correspond to high vegetation, while downspikes indicate water. Mark 1 coincides with scattered green vegetation observed on video. This feature is also visible in the PRT-5 time series by a slightly smaller surface temperature than the surrounding. In the area of Mark 2 sparse vegetation is predominant. Mark 3 shows a creek, surrounded by vegetation. These characteristics cannot be resolved by the PRT5 instrument. In this time series irrigated green farmland with a high maximum vegetation index of 0.78 is resolved at Mark 4. Again, this vegetation peak is inverted to the surface temperature. The wide Mark 5 shows the diversity in the South Platte River area, Colorado. The Riverside Reservoir surrounded by lush vegetation can clearly be seen at Mark 6. Even some structure within the Riverside Reservoir is resolved, suggesting the presence of algae in the lake.

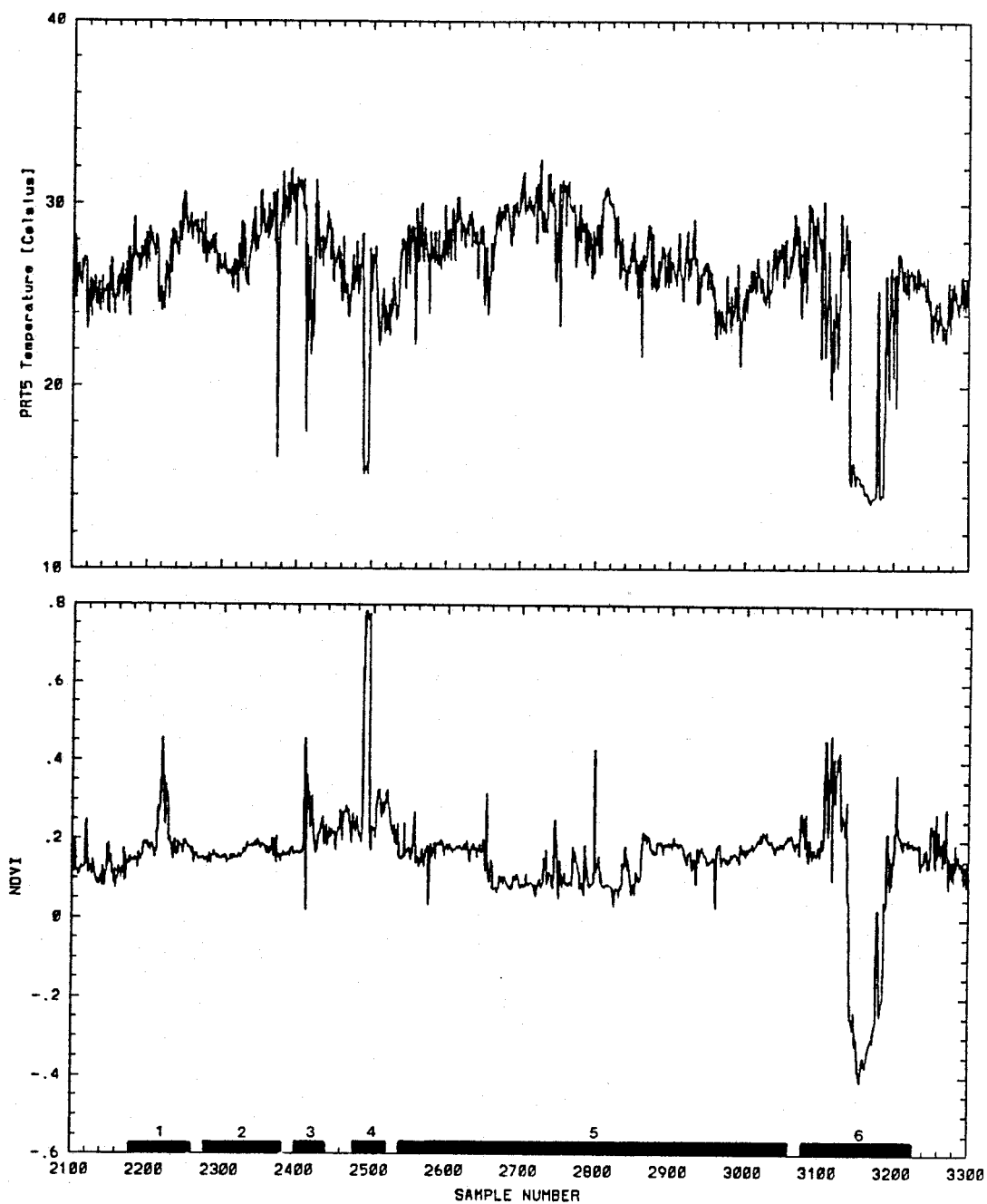


Fig. 4.1 Time series of the radiometrically measured surface temperature and derived vegetation index NDVI in the Greely area, Colorado.

To show more detail of the vegetation index, the section between samples number 2340 and 2580 of Figure 4.1 is presented at 25 Hz rate data in Figure 4.2. This corresponds to a time interval of 240 sec or, if expressed in distance, of about 20.9 km. When looking at this figure, it should be remembered that the SVR data are filtered at 10 Hz. The PRT-5 data are not shown in this case because the data were filtered at 1 Hz and cannot be compared directly. At Mark 1 the video recording shows an almost dried out creek with little vegetation around it. The video image coincides with a weak NDVI signal. A much stronger effect is visible at Mark 2 of this figure. Here the video reveals a river surrounded by lush vegetation with an NDVI above 0.5. Further along at Mark 3 is irrigated farmland with extremely green vegetation and values for NDVI of almost 0.8. The width of the irrigated farmland is estimated to be 650 m. Between the marks dry, sparsely vegetated farmland in this area is indicated with a vegetation index between 0.18 and 0.3.

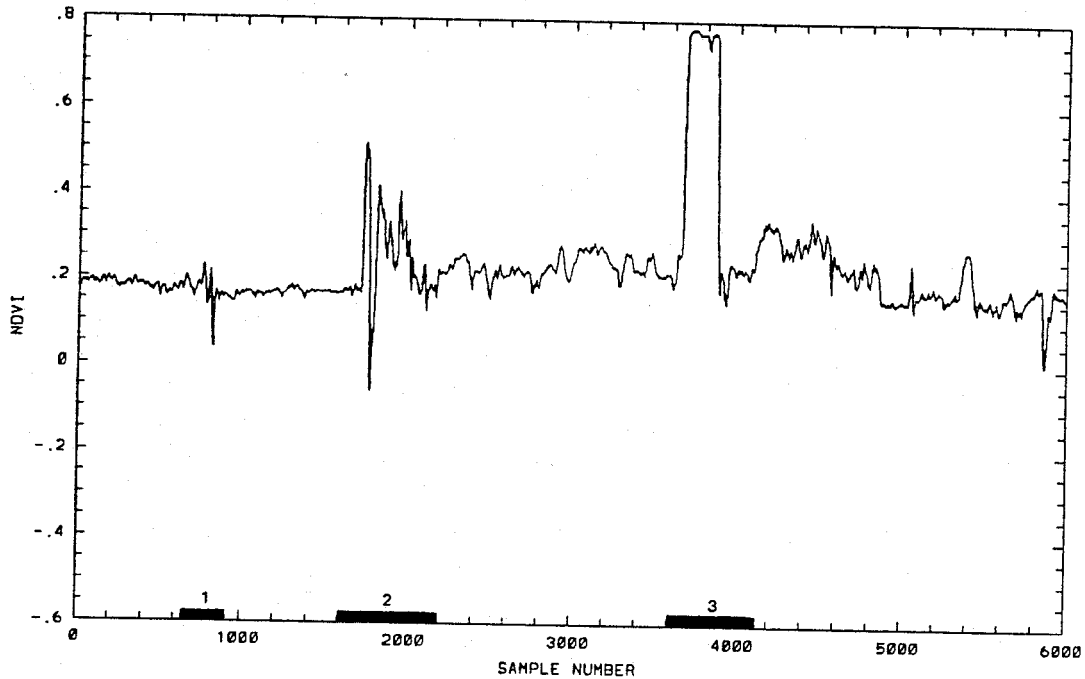


Fig. 4.2 High rate vegetation index time series.

A high-rate vegetation index time series of the Riverside Reservoir, Colorado and vicinity can be seen in Figure 4.3. This example shows the potential of the SVR to those other than atmospheric scientists. The Riverside Reservoir can be seen in the middle surrounded by vegetation. The cross section of the reservoir is about 4.1 km. A minimum value of the NDVI within the lake was observed to be -0.4. Generally, when measuring the vegetation index over water one can expect a constant negative value. In the presented case, however, we explicitly see a variation of the NDVI within the reservoir. This feature was caused by

greenish algae and was verified by the video image. Further investigations are required to validate the usefulness of the airborne vegetation radiometer as a detection system for algae on water. Different wavelengths might be required to better detect the presence of algae. Close to the edge of the reservoir a sand bank is indicated by a wide spike in the NDVI on the marked section of the time series.

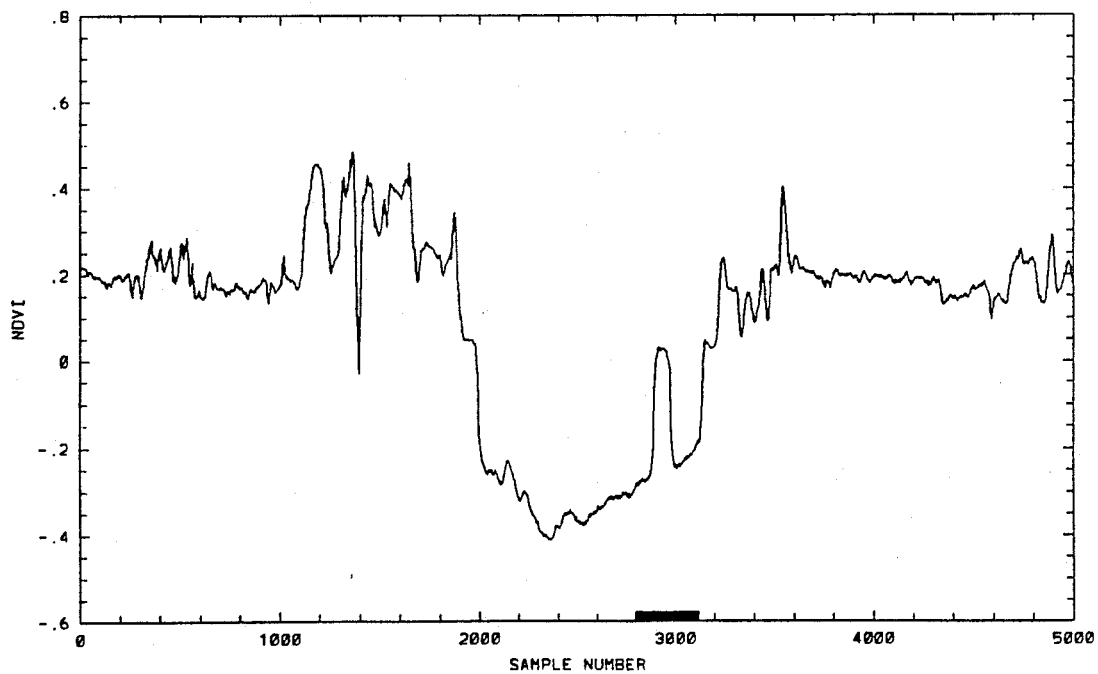


Fig. 4.3 High rate NDVI time series of the Riverside Reservoir, Colorado.

A further application of the VEG2 radiometer is the detection of shade on the ground projected by clouds. The shaded areas of the underlying ground transforms the latent and sensible heat fluxes. The NDVI, the 650 nm signal and the 862 nm signal are plotted in Figure 4.4. One sample in the graph is equivalent to one second. The whole section of the flight, hence, corresponds to 45 minutes. A high variability of the vegetation index can be seen between the samples number 4200 to 4450 and 6350 to 6900. Between data points 4450 and 6350 the variation in the NDVI is small. The drop in the individual signal of the wavelengths 650 and 862 nm at sample number 5350 to 5800 indicates an area shaded by clouds. This feature was verified by the video image. Thus, by calculating the NDVI and correlating the absolute value of the received radiance signal from the detector, the projected shadow of clouds can be identified. Furthermore, this example shows that the retrieved vegetation index is independent of any cloud cover.

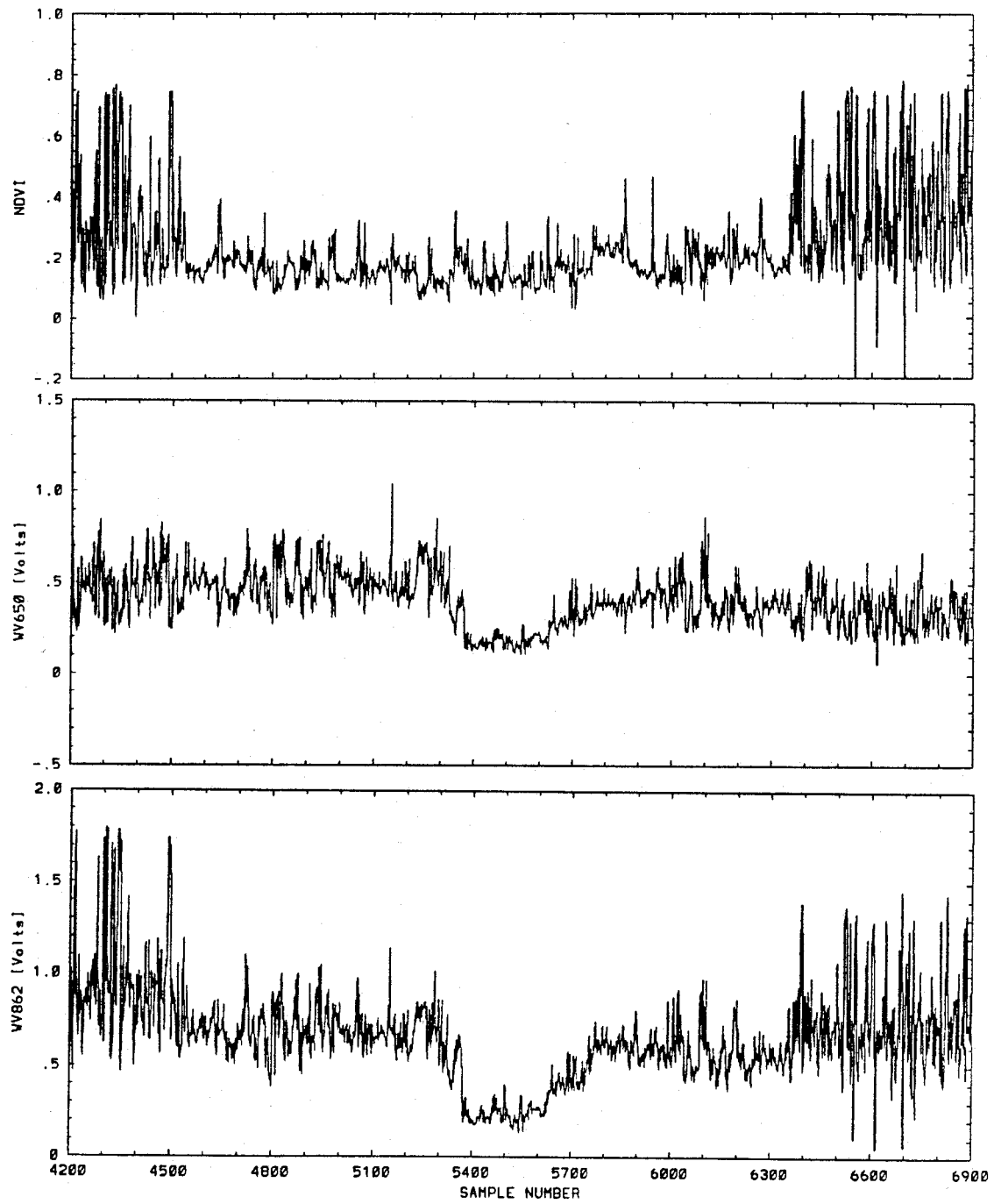


Fig. 4.4 Example of data from the vegetation radiometer, identifying shade projected by clouds.

5 SUMMARY

The construction of the spectral vegetation radiometer SVR operated on the NCAR King Air Beechcraft aircraft is simple. The calibration procedure was described in detail. The lack of need for an absolute radiance calibration makes it possible to use the ratio-Langley technique. From the SVR the vegetation parameter was derived from the observed radiance signals and not from the reflectances as usually accomplished from satellite data. This approach circumvents a second upward-facing radiometer installed on the aircraft, necessary to determine the reflectance, and the complex correction for aircraft maneuvers during the observations. Utilizing the vegetation radiometer within the boundary layer minimizes the influence of atmospheric constituents which is significant for observations from high altitudes.

The fast response allows the resolution of even single trees when flying low, and cloudy conditions do not pose a problem. The examples given demonstrate the potential of the spectral vegetation radiometer for micro-meteorological studies in the planetary boundary layer.

Currently a classification technique is under development, using the derived NDVI and the individual wavelength signals as a basis to group different types of surfaces. This indicator function, has in contrast to the determination of an absolute value of the vegetation index, the advantage that the dependencies of the radiance signals of the sun-target-sensor geometry are avoided.

REFERENCES

- Bannehr, L., 1990: *Airborne Spectral Radiation Measurements in South Australia*, Ph.D. Thesis, Flinders University of South Australia, 180 pp.
- Blümel, K., Bolle, H.J., Eckhardt, M., Lesch, L., Tonn, W., 1988: *Der Vegetationsindex für Mitteleuropa 1983 - 1985*, Institut für Meteorologie der Freien Universität Berlin
- Bolle, H.J., 1990: *Vegetationsindices*, promet, Fernerkundung in der Meteorologie I, 105-113
- EG&G Judson, 1990: Silicon Photodiodes, Catalog
- Forgan, B.W., 1988: *Determination of aerosol optical depth at sea level station - investigation at Cape Grim BAPS*, Cape Grim Baseline Air Pollution Station, Technical Report 5, 70
- Forgan, B.W., 1988: *Sunphotometer calibration by the ratio-Langley method*, Baseline Atmospheric Program (Australia) 1986, eds. B.W. Forgan and P.J. Fraser, Bureau of Meteorology, Melbourne, 22-26
- Fröhlich, C. and London, J. (ed.), 1986: *Revised Instruction Manual on Radiation Instruments and Measurements*, WCRP Publication Series No. 7, WMO/TD-No. 149
- Hope, A.S. and McDowell, T.P., 1990: *The use of remotely sensed surface temperature and a spectral vegetation index for evaluating heat fluxes over Konza prairie*, Symposium on the First ISLSCP Field Experiment (FIFE), Feb. 7-9, 1990, Anaheim, Calif., American Meteorological Society
- Kasten, F., 1966: A New Table and Approximation Formula for the Relative Optical Air Mass, *Arch. Meteor. Geoph. Biocl., Ser. B*, 14, 206-223
- Omega Optical, 1990: *Interference Filters and Coating*, Brattleboro, Vermont 05301
- Paltridge, G.W. and Barber, J., 1988: Monitoring Grassland Dryness and Fire Potential in Australia with NOAA/AVHRR Data, *Remote Sensing of Environment*, 25, 381-394
- Robinson, G.D, 1966: *Solar Radiation*, Elsevier Publishing Company, Amsterdam, 347 pp.
- Sellers, P.J., 1985: Canopy Reflectance, Photosynthesis and Transpiration, *Int. J. Remote Sensing*, 6, 1335-1372
- Tucker, C.J., Fung, I.Y., Keeling, C.D. and Gammon, R.H., 1986: Relationship between atmospheric CO₂ variations and a satellite-derived vegetation index, *Nature*, 319, 195-199

APPENDIX A

VEGCAL program


```

      call erro('   Array "n" in program VEGCAL is too small !!')
    end if

      read(iread,*,err=500,end=700) time(i), (direct(i,j),j=1,m)

      do 30, j=1,m
        direct(i,j) = direct(i,j) - offs(j)
        xx(i,j) = log(direct(i,j))
30      continue

      goto 510

700    ien=i-1
        iele = ien

c    reading completed

      close(iread)

c    reorder measurements if readings were taken in the morning

      if(xx(1,1).lt.xx(ien,1)) then
        do 90,i=1,ien
          x1(i,1) = xx(ien+1-i,1)
          x1(i,2) = xx(ien+1-i,2)
          x1(i,3) = xx(ien+1-i,3)
          til(i) = time(ien+1-i)
90      continue

        do 95,i=1,ien
          xx(i,1) = x1(i,1)
          xx(i,2) = x1(i,2)
          xx(i,3) = x1(i,3)
          time(i) = til(i)
95      continue
        end if

c    calculate solar elevation, refraction and air mass

      ian = 1

      do 50, j=1,m
        ien = iele
        do 10,i=ian,ien

          call zenith(time(i), year, month, day, lat, long, zone, az, so, decl, gha)

c    calculate refraction

      refr = 0.25 / (exp(feet/27000.) * tan(so/60))
      a = int(refr * 100.) / 60.
      b = (refr - int(refr * 100.) / 100.) / 0.36
      refr = (a + b) / 10.

      so = so + refr

```

```

      call airmas(so,airm)

      sair(i) = airm(1)
      ws(i) = airm(2)
      op(i) = airm(3)

      oml(i) = (airm(1) + airm(2) + airm(3)) / 3.

c    find limits (air mass 2 to 6) for determination of the cal coef.

      if(oml(i).lt.om_11) ian = i
      if(oml(i).lt.om_12) ien1 = i

10    continue

      ien = ien1
      a_mass1 = oml(ian)
      a_mass2 = oml(ien)

c    shovel data to limits set for air mass 1 and 2

      do 12,i=ian,ien
        ii = i - ian + 1
        oml(ii) = oml(i)
        sair(ii) = sair(i)
        ws(ii) = ws(i)
        op(ii) = op(i)

        direct(ii,j) = direct(i,j)
        xx(ii,j) = xx(i,j)

12    continue

      ien = ien - ian + 1

c    remove linear trend before rejecting data exceeding a certain specified
c    standard deviation

      do 69,i=1,ien
        x1(i,j) = xx(i,j)
69      continue

c    co(1) = intercept, co(2) = slope

      call dlinstats(ien,oml,xx(1,j),co,sse,sx,sy,se,con,rs,ierr)

      do 72,i=1,ien
        x1(i,j) = xx(i,j) - (x1(i,j)*co(2) - co(1))

      call reject(x1(1,j),xx(1,j),oml,n,ien,thres)

      if(j.eq.1) then
        ien650 = ien
        wv = 0.65
        tau_oz = 0.021
      end if

```

```

if(j.eq.2) then
  ien760 = ien
  wv = 0.760
  tau_oz = 0.00195
end if

if(j.eq.3) then
  ien862 = ien
  wv = 0.862
  tau_oz = 0.
end if

c calculate molecular optical depth. equation after Frohlich and Shaw (1980)
c and corrected by Young (1980).

tau_mol = p/p0*0.0088641*wv**(-(3.916+0.074*wv+0.05/wv))

call dlinstats(ien,oml,xx(1,j),co,sse,sx,sy,se,con,rs,ierr)

tau_tot = abs(co(2))

c calculate weighted air mass oml

do 35,i=1,ien
  tau_aer = tau_tot - tau_mol - tau_oz
  oml(i) = (sair(i)*tau_mol+op(i)*tau_oz+tau_aer*ws(i)) /
6 tau_tot
35 continue

c use weighted air mass to compute V0_ls and tau_ls (least squares method)

call dlinstats(ien,oml,xx(1,j),co,sse,sx,sy,se,con,rs,ierr)

V0_ls(j) = exp(co(1)) / rv ! / rv converts to 1 AU
tau_ls(j) = abs(co(2))
sdev(j) = se

c open output file and store air mass as well as ln(signal)
c of individual wavelengths

if(j.eq.1) vegout = 'veg650.out'
if(j.eq.2) vegout = 'veg760.out'
if(j.eq.3) vegout = 'veg862.out'

open(60,file=vegout)

do 60,i=1,ien
  write(60,111) oml(i), xx(i,j)
60 continue
close (60)

50 continue

111 format(f6.3,f7.4)

```

```

c calculate ratio Langley factors
c12 = ((E0650/E0760) / (V0_ls(1)/V0_ls(2)))
c32 = ((E0862/E0760) / (V0_ls(3)/V0_ls(2)))

c print results to the screen
444 write(6,'(///,10x,a)') 'RESULTS OF THE CALIBR
&A T I O N'
write(6,'(10x,a,/)' ) '-----'
&-----'

write(6,'(26x,a,i2,a,i2,a,i4)') 'Date = ',day,'/',month,'/
&',year

write(6,'(20x,a,f7.2)') ' Longitude = ',long
write(6,'(20x,a,f6.2)') ' Latitude = ',lat
write(6,'(20x,a,f5.3)') ' Air mass a = ',a_mass1
write(6,'(20x,a,f5.3)') ' Air mass b = ',a_mass2
write(6,'(20x,a,i4,/)' ) 'Total Observations = ',icle

write(6,'(20x,a)') 'Least Squares Analysis'
write(6,'(16x,a,/)' ) 'Individual Calibration Factors'
write(6,'(20x,a,i4)') 'Observations : ',ien650
write(6,'(20x,a,f7.2)') 'V0_650 : ',V0_ls(1)
write(6,'(20x,a,f7.5)') 'tau_650 : ',tau_ls(1)
write(6,'(20x,a,f7.4,/)' ) 'sdev_650 : ',sdev(1)

write(6,'(20x,a,i4)') 'Observations : ',ien760
write(6,'(20x,a,f7.2)') 'V0_760 : ',V0_ls(2)
write(6,'(20x,a,f7.5)') 'tau_760 : ',tau_ls(2)
write(6,'(20x,a,f7.4,/)' ) 'sdev_760 : ',sdev(2)

write(6,'(20x,a,i4)') 'Observations : ',ien862
write(6,'(20x,a,f7.2)') 'V0_862 : ',V0_ls(3)
write(6,'(20x,a,f7.5)') 'tau_862 : ',tau_ls(3)
write(6,'(20x,a,f7.4,/)' ) 'sdev_862 : ',sdev(3)

write(6,'(20x,a)') 'Ratio Langley Calibration'
write(6,'(6x,a,/)' ) 'These factors must be multiplied by the 650 a
&nd 862 nm signals'
write(6,'(20x,a,f7.4)') 'C_650 : ',c12
write(6,'(20x,a,f7.4,/)' ) 'C_862 : ',c32

stop
end

```

```

      subroutine zenith(td,year,mon,iday,lat,long,zone,az,so,decl,gha)
cccccccccccccccccccccccccccccccccccccccccccccccccccccccccccccccccccc
c
c   calculates local azimuth and zenith distance for specified
c   location and time using approximations to nautical almanac
c   td= time in 24 hours (hhmm.ss)
c   year = year number (eg 1977)
c   mon = month of year
c   iday = day of month
c   lat = latitude in degrees and decimal (ex. -34.75)
c   long = longitude in degrees and decimal (ex. 138.75)
c   zone = zone time from greenwich in fractions of hours (ex. -9.5)
c   az = azimuth of sun in degrees (postive east of south)
c   e = zenith distance of sun in degrees
c   so = solar elevation
c   gha = greenwich hour angle of sun in degrees west of greenwich
c   decl = declination of the sun in degrees ( north +ve )
c
c   this program was taken from r.walraven(1978) and archer(1980)
c   additional code and differnt format was done by forgan(1980)
c
c   changes of different latitude and longitude format as well as
c   exact conversion of the time (hhmm.ss) to time decimal was done
c   by lb
c
c   updated : 18/1/91   lb
cccccccccccccccccccccccccccccccccccccccccccccccccccccccccccccccccccc
      real lat,long,long1
      integer year,day
      real*8 mm,mmd,mmss,hhmmss,ssd,ss
      data twophi, rad /6.2831853,0.017453293/

      long1 = long
      if(long.gt.0..and.long.lt.180.) long=360.-long
      if(long.lt.0) long =abs(long)

c   conversion of time (hhmm.ss) into decimal time

      t = td * 1.e2
      hhmmss = dble(t)
      mmss = (hhmmss/1.d4 - int(hhmmss/1.d4)) + 1.d-7
      ss = (mmss*1.d2 - int(mmss*1.d2))/1.d2
      mm = int(mmss*1.d2)/1.d2
      mmd = mm/.6
      ssd = ss/.36
      t = int(hhmmss/1.d4) + mmd + ssd

c   conversion end

      i = 1
      j = iday
      b=0.5
      k=0

```

```

      if (mon.lt.3 ) goto 10
      i=3
      b=59.5
      x=year/4.0
      k= ifix (x-ifix(x-0.1))
10 p=mon-i
      l=ifix(p*30.6 +b)
      day = j + k + 1
      delyr= year -1980.
      leap = ifix (delyr/4.)
      t = t + zone
      time=delyr*365. + leap +day - 1. +t/24.
      if (delyr .eq. leap*4.) time =time -1.
      if((delyr.lt.0.0).and.(delyr.ne.leap*4.0)) time= time -1.
      theta =(360.*time/365.25) *rad
      g = -0.031271 -4.53963e-7*time + theta
      e1 = 4.900968 +3.67474e-7*time
      el=e1+(0.033434-2.3e-9*time)*sin(g)
      el=e1 + 0.000349*sin(2.*g) + theta
      eps = 0.409140 -6.2149e-9*time
      sel = sin(el)
      a1 = sel* cos(eps)
      a2 = cos(el)
      ra = atan2(a1,a2)

      if(ra.lt.0.) ra=ra+twophi

      decl =asin(sel*sin(eps))
      st= 1.759335 +twophi*(time/365.25 -delyr)
      st= st + 3.694e-7*time
      if (st.ge.twophi) st= st -twophi
      s= st -long*rad +rad*15.0*t
      if (s.ge.twophi) s = s - twophi
      h= ra -s
      phi = lat*rad
      e = sin(phi)*sin(decl) + cos(phi)*cos(decl)*cos(h)
      e=asin(e)
      a = cos(decl)*sin(h)/cos(e)
      if(abs(a).gt.1.00000) a = sign(1.00000000,a)
      a=asin(a)/rad
      if (sin(e).ge.sin(decl)/sin(phi)) goto 100
      if (a.lt.0.) a= a + 360.
      a= 180. - a
100 e = 90. - e/rad
      h = h/rad
      h= amod(h,360.)
      if (h.lt.0.0) h= 360.+h
      gha = long - h
      gha= amod(gha,360.)
      if (gha.lt.0.0) gha = gha + 360.
      decl=decl/rad
      az = a
      so = 90 - e
      long = long1

      return
      end

```

```

      subroutine DLINSTATS(n,x,y,co,sse,sx,sy,se,con,rs,ierr)
c Debug History
c Created: 8 Dec 1988 from LINSTATS - first deletes the means
c   of x and y in double precision, before calculating
c   the statistics. More operations but less subtraction
c   of small resultant quantities.

c Inputs
c n = number of pairs of x and y
c x = array of n points
c y = array of points regressed against x

c Output
c co(1) = intercept of straight line regression
c co(2) = slope of the regression line

c sse = standard error estimate
c sx = error estimate in x
c sy = error estimate in y
c se = unbiased estimate of standard deviation

c con(1) = confidence multiplier for the intercept
c con(2) = confidence multiplier for the slope

c rs = sample coefficient of determination
c   ( correlation coefficient squared)
c ierr = 0 then OK
c       = 3 then not enough points

      integer n,ierr
      real x(n),y(n),co(2),con(2),rs,se,sse,sx,sy

c Local variables
      real*8 dxm,dxm,dym,dco2,dxx,dyy,dxm,dym,dxa,dya,dsse,dse
      real*8 dn,dnm1,dnm2,dzero

c Dot products
      ierr = 3
      if(n.lt.3) return
      ierr = 0
c Convert to double precision
      dzero = 0.000000d00
      dxm = dzero
      dym = dzero
      dn = dfloat(n)
      dnm1 = dfloat(n-1)
      dnm2 = dfloat(n-2)

      do 10 i = 1,n
         dxm = dxm + dble(x(i))
         dym = dym + dble(y(i))
10      continue
      dxm = dxm / dn ! mean x
      dym = dym / dn ! mean y

      dxx = dzero
      dyy = dzero
      dxy = dzero

      do 20 i = 1,n
         dxa = dble(x(i)) - dxm
         dya = dble(y(i)) - dym
         dxx = dxx + dxa * dxa
         dyy = dyy + dya * dya
         dxy = dxy + dxa * dya
20      continue

c Slope calculation
      dco2 = dxy/dxx
      co(2) = dco2

c Intercept calculation
      co(1) = dym - dco2 * dxm

c Standard error estimate
      dsse = dyy - dco2 * dco2 * dxx
      sse = dsse

c Standard deviation estimate from unbiased estimate
      dse = dabs(dsse / dnm2)
      se = dsqrt(dse)
      dsx = dabs(dxx) / dnm1
      dsy = dabs(dyy) / dnm1
      dsx = dsqrt(dsx)
      dsy = dsqrt(dsy)
      sx = dsx
      sy = dsy

c Sample coefficient of determination
      rs = dco2 * dco2 * dxx / dyy

c Confidence limits on intercept
      con(1) = dse / dsqrt(dn)

c Confidence multiplier on slope
      con(2) = dse / (dsx + dsqrt(dnm1))

      return
      end

```

```

subroutine rejec1(aa,bb,cc,nn,iele,thres)
cccccccccccccccccccccccccccccccccccccccccccccccccccccccccccc
c
c purpose: rejects data from time series which are greater than
c thres* standard deviation. The time series is shorten
c
c author: lb
c
c updated: 18/9/91
cccccccccccccccccccccccccccccccccccccccccccccccccccccccccccc

parameter(mm=1000)
real aa(nn),bb(nn),cc(nn),xx(mm),yy(mm),zz(mm)

if(iele.gt.mm) then
print*, 'iele=',iele,'mm=',mm
call erro('iele.gt.MM in Sub REJEC1 ! ')
end if

c computing mean

iele=iele
sdvl=1.e20
111 sum=0.

do 10,i=1,ien
10 sum=sum+aa(i)
xmean=sum/ien

if(ien.eq.0) call erro(' Division by zero error in Sub REJEC1 ! ')

c computing standard deviation

sum=0.
do 20,i=1,ien
20 sum=sum+((xmean-aa(i))*(xmean-aa(i)))
xsd=sqrt(sum/(ien-1))

c selection of values in time series less then thres*sdv

c=thres*xsd+xmean
cl=xmean-(thres*xsd)

k=0
do 100,i=1,ien

if((aa(i).lt.c).and.(aa(i).gt.cl)) then
k=k+1
yy(k)=aa(i)
xx(k)=bb(i)
zz(k)=cc(i)
end if

```

```

100 continue

do 110,i=1,ien
bb(i)=xx(i)
cc(i)=zz(i)
110 aa(i)=yy(i)

sdvfac=sdvl/xsd

if (sdvfac.gt.1.01) then
sdvl=xsd
ien=k

if(ien.lt.2) call erro(' All numbers in REJEC1 rejected ! ')

goto 111
end if

iele=ien

return
end

```

```
function sradii(day,mon)
```

```

c calculates earth-sun radius parameter from irradiance calculations
c day,mon are the day and month of the year
c sradii = ((radius mean)/(radius(day,mon))) squared
c hence solar input(day,month) = sradii* solar constant

```

```

integer day
dimension month(12)
data month/0,31,59,90,120,151,181,212,243,273,304,334/
x = month(mon) + day
if (x.gt.365.) x = 1.0
th = x*6.283185307/365.
s = 1.000110+0.034221*cos(th) + 0.001280*sin(th)
th2 = th*2.0
s = s + 0.000719*cos(th2) + 0.000077*sin(th2)
sradii = s

```

```

return
end

```

